HHS Public Access

Author manuscript

Brain Behav Immun. Author manuscript; available in PMC 2018 October 01.

Published in final edited form as:

Brain Behav Immun. 2017 October ; 65: 210–221. doi:10.1016/j.bbi.2017.05.004.

HIV-1 Tat protein enhances sensitization to methamphetamine by affecting dopaminergic function

James P. Kesby[1,2], **Julia A. Najera**[3], **Benedetto Romoli**[1], **Yiding Fang**[3], **Liana Basova**[3], **Amanda Birmingham**[4], **Maria Cecilia G. Marcondes**[3,*,#], **Davide Dulcis**[1,*,#], and **Svetlana Semenova**[1,*,#]

[1]Department of Psychiatry, School of Medicine, University of California San Diego, La Jolla, CA, USA

[2]Queensland Brain Institute, The University of Queensland, St. Lucia, Qld, Australia

[3]Department of Molecular and Cellular Neurosciences, The Scripps Research Institute, La Jolla, CA, USA

[4]Center for Computational Biology and Bioinformatics, University of California San Diego, La Jolla, CA, USA

Abstract

Methamphetamine abuse is common among humans with immunodeficiency virus (HIV). The HIV-1 regulatory protein TAT induces dysfunction of mesolimbic dopaminergic systems which may result in impaired reward processes and contribute to methamphetamine abuse. These studies investigated the impact of TAT expression on methamphetamine-induced locomotor sensitization, underlying changes in dopamine function and adenosine receptors in mesolimbic brain areas and neuroinflammation (microgliosis). Transgenic mice with doxycycline-induced TAT protein expression in the brain were tested for locomotor activity in response to repeated methamphetamine injections and methamphetamine challenge after a 7-day abstinence period. Dopamine function in the nucleus accumbens (Acb) was determined using high performance liquid chromatography. Expression of dopamine and/or adenosine A receptors (ADORA) in the Acb and caudate putamen (CPu) was assessed using RT-PCR and immunohistochemistry analyses. Microarrays with pathway analyses assessed dopamine and adenosine signaling in the CPu. Activity-dependent neurotransmitter switching of a reserve pool of non-dopaminergic neurons to a dopaminergic phenotype in the ventral tegmental area (VTA) was determined by immunohistochemistry and quantified with stereology. TAT expression enhanced methamphetamine-induced sensitization. TAT expression alone decreased striatal dopamine (D1,

*Corresponding Authors: Drs. Semenova and Dulcis, Department of Psychiatry, M/C 0603, School of Medicine, University of California San Diego, 9500 Gilman Drive, La Jolla, CA 92093-0603, USA. ssemenova@ucsd.edu (SS); ddulcis@ucsd.edu (DD). Dr. Marcondes currently with San Diego Biomedical Research Institute, 10865 Road to Cure, Suite 100, San Diego, CA 92121, USA. cmarcondes@SDBRI.ORG.

#senior co-authors

The authors declare no competing financial interests.

D2, D4, D5) and ADORA1A receptor expression, while increasing ADORA2A receptors expression. Moreover, TAT expression combined with methamphetamine exposure was associated with increased adenosine A receptors (ADORA1A) expression and increased recruitment of dopamine neurons in the VTA. TAT expression and methamphetamine exposure induced microglia activation with the largest effect after combined exposure. Our findings suggest that dopamine-adenosine receptor interactions and reserve pool neuronal recruitment may represent potential targets to develop new treatments for methamphetamine abuse in individuals with HIV.

Keywords

TAT expression; locomotor activity; dopamine receptors; adenosine receptors; brain neurochemistry; HPLC; gene expression microarrays; neurotransmitter respecification; mice

1. Introduction

There is a high prevalence of methamphetamine abuse in HIV+ humans ranging between 40–60% (Rajasingham et al. 2012; Shoptaw et al. 2003). Neurotoxic effects of methamphetamine and HIV disease on the brain are well documented (Ferris et al. 2008; Purohit et al. 2011). However, studies on the brain adaptations that occur during early stages of methamphetamine use and HIV infection are uncommon.

Methamphetamine reward is largely mediated by the dopaminergic system in corticolimbic brain areas including the medial prefrontal cortex (mPFC), nucleus accumbens (Acb), and ventral tegmental area (VTA) (Koob and Volkow 2010). HIV infection has been associated with impaired dopamine function in the basal ganglia (Kumar et al. 2011) and excessive glutamatergic function in frontal lobes (Nagarajan et al. 2012). Thus, dopamine and glutamate transmitter systems in corticolimbic circuits may be differentially affected in HIV + subjects and alter sensitivity to methamphetamine.

HIV viral products may contribute to neuropathology, reward deficits and drug dependence in treated patients (Merino et al. 2011). The viral TAT (trans-activator of transcription) protein is found in the central nervous system of HIV+ humans, even when serum CD4 levels are normalized with antiretroviral drugs (Mediouni et al. 2012). Transgenic mice that express the TAT protein in the brain, under the glial fibrillary acidic protein (GFAP) promoter and inducible by treatment with doxycycline, show neuropathology that is similar to that observed in HIV-infected humans (Kim et al. 2003), therefore providing a useful *in vivo* model to study the temporal impact of TAT protein on brain function. Moreover, TAT-induced dysfunction in corticolimbic dopaminergic neurotransmission (Ferris et al. 2009; Kesby et al. 2016b; Midde et al. 2012; Theodore et al. 2012; Zhu et al. 2009) may lead to alterations in reward function (Kesby et al. 2016b; Koob and Volkow 2010). We have previously shown that the expression of HIV-associated proteins, such as gp120 and TAT, increase the sensitivity to methamphetamine reward (Kesby et al. 2016b; Kesby et al. 2014).

The present studies investigated how HIV-1 TAT expression in the brain impacted dopamine and modified the reward function during methamphetamine-induced locomotor sensitization. Locomotor sensitization is the augmented motor-stimulant response after a period of

abstinence that occurs with repeated, intermittent administration of psychostimulants. Such a phenomenon is thought to reflect aspects of the neuronal adaptations underlying drug dependence (Robinson and Berridge 2008), and mediated by both mesolimbic and mesocortical circuits (Steketee 2003).

We also determined the activity-dependent induction of neurotransmitter re-specification within a reserve pool of non-dopaminergic neurons to a dopaminergic phenotype in the ventral mesencephalon using quantification of the numbers of tyrosine hydroxylase (TH) - positive neurons (Dulcis and Spitzer 2008). Activity-dependent homeostatic plasticity in the brain involves changes in synaptic strength, number of synapses, neuronal excitability (Dulcis and Spitzer 2012; Nelson and Turrigiano 2008) and neurotransmitter expression (Dulcis et al. 2013). The presence of a reserve pool of neurons that can boost function of an endogenous circuit has been proposed as a novel mechanism of neuroplasticity (Dulcis and Spitzer 2012; Lewis et al. 2014; Velazquez-Ulloa et al. 2011). Indirect evidence for activity-dependent recruitment of a new population of neurons in amphetamine-sensitized rats (Nordquist et al. 2008) suggests this phenomenon may also be a feature in the development of psychostimulant abuse.

Further, monoamine, glutamate and GABA function in the Acb was determined using high performance liquid chromatography (HPLC). The impact of TAT and methamphetamine on gene expression profile was determined in the brain tissue using microarrays followed by a pathway analyses with a focus on dopamine signaling in the caudate putamen (CPu). Levels of dopamine receptors (DRD) and adenosine receptors (ADORA), that are co-expressed in the basal ganglia (Ferre et al. 1997) and involved methamphetamine reward (Chesworth et al. 2016; Kavanagh et al. 2015; Pierce and Kalivas 1997; Shimazoe et al. 2000), were assessed and validated in the Acb and CPu using RT-PCR and immunohistochemistry (IHC) analyses. Finally, we also evaluated neuroinflammatory processes in the CPu by assessing expression of the ionized calcium binding adaptor molecule 1 (IBA-1), a marker for microglial activation (microgliosis).

2. Materials and methods

2.1. Animals

A total of 82 male mice (3–5 months old), with 43 containing the GFAP promotor-controlled Tet-binding protein (TAT−) and 39 containing both the GFAP promotor-controlled Tet-binding protein and the TRE promotor-TAT protein transgene (TAT+) were tested. Inducible TAT transgenic mouse colonies with a C57BL/6J background were obtained by generation of two separate transgenic lines Teton-GFAP mice and TRE-Tat86 mice, and then cross-breeding of these two transgenic mouse lines, as previously described (Kim et al. 2003). The mice were housed in groups of 2–4 in a humidity- and temperature-controlled animal facility on a 12 h/12 h reverse light/dark cycle (lights off at 7:00 AM) with *ad libitum* access to food and water. Behavioral testing was conducted during the dark phase of the light/dark cycle from 8 AM to 7 PM with mice from all groups being tested concurrently at any given time throughout the testing period. All of the experiments were conducted in accordance with the guidelines of the American Association for the Accreditation of Laboratory Animal Care and National Research Council's Guide for the Care and Use of Laboratory Animals and

approved by the University of California San Diego Institutional Animal Care and Use Committee.

2.2. Locomotor activity testing

Locomotor activity was assessed in four open field arenas (60 × 60 cm) equipped with infrared beams (Med Associates, St. Albans, VT, USA) to calculate total distance travelled. Mice were acclimatised to the testing room at least one hour prior to testing and were tested in the dark for a total of 30 min.

2.3. Doxycycline regimen

All mice were treated with a doxycycline regimen (doxycycline hyclate; Sigma) of 100 mg/kg, intraperitoneally, once a day for 7 days. This regimen is based on the previously demonstrated efficacy of TAT induction at this dose of doxycycline (Carey et al. 2012; Paris et al. 2014a). Doxycycline-induced TAT expression was attenuated by day 7 and significantly decreased 14 days after the termination of doxycycline treatment (Paris et al. 2014a). Only mice containing both the GFAP promotor-controlled Tet-binding protein and the TRE promotor-TAT protein transgene (TAT+) generate TAT protein after doxycycline administration. Mice were administered doxycycline injections in the evening (17:00h), beginning the day before the methamphetamine acquisition phase.

2.4. Methamphetamine sensitization

The sensitization procedure consisted of an acquisition phase with seven consecutive days of locomotor testing directly after an intraperitoneal injection with either saline (0.9%) or 2 mg/kg methamphetamine (methamphetamine hydrochloride; Sigma, St. Louis, MO, USA). The challenge phase occurred after a seven-day washout period. Mice were tested after either saline or 1 mg/kg methamphetamine. The methamphetamine doses were selected based on the literature (Jing et al. 2014). There were four testing groups: saline acquisition and saline challenge (SAL/SAL), methamphetamine acquisition and saline challenge (METH/SAL), saline acquisition and methamphetamine challenge (SAL/METH), methamphetamine acquisition and methamphetamine challenge (METH/METH).

2.5. Neurochemical and molecular analyses

Mice were euthanized via cervical dislocation 30 minutes after completing the locomotor challenge (1 h after injections of SAL/METH). Brain samples were rapidly dissected and samples frozen on dry ice and stored at −80°C until analysis. In a subgroup of these mice (n=5), from the SAL/METH and METH/METH groups, sample from one hemisphere were used for Bioinformatics (CPu) and PCR (Acb) studies. A separate subset of mice (n=4) from the SAL/METH and METH/METH groups were perfused 24 h after the locomotor challenge for dopamine cell counting in the SN and VTA.

2.6. High performance liquid chromatography and analysis

Catecholamines and amino acids from brain tissue were measured by high performance liquid chromatography with electrochemical detection for catecholamines and fluorescence detection for amino acids (Groves et al. 2013; Kesby et al. 2016a, c; Kesby et al. 2009).

Brain tissues were homogenized in 0.1 M perchloric acid with 50 ng/mL deoxyepinephrine (catecholamine internal standard) using probe sonication (Vibra-Cell, Sonics & Materials, CT, USA) and centrifuged at 13,000 rpm for 5 min. The supernatant was filtered with a 4 mm 0.22 μM nylon syringe filter (MicroSolv Technology Corporation, NJ, USA). For catecholamines, 15 μL of sample was injected into the HPLC system, which consisted of an autosampler (Dionex UltiMate 3000, Thermo Scientific, CA, USA), an isocratic HPLC pump (Model 584, ESA Laboratories, MA, USA), a Sunfire C18 column, (4.6 mm × 100 mm, 3 um; Waters Corporation, MA, USA) and a Coulochem III (ESA Laboratories) electrochemical detector. The mobile phase consisted of a 12% acetonitrile/50 mM citric acid and 25 mM potassium dihydrogen phosphate buffer containing 1 mM EDTA and 1.4 mM octane sulfonic acid adjusted to pH 4.3 with phosphoric acid. Flow rate was 0.5 ml/min. An analytical cell (Model 5014B, ESA Laboratories) with the first and second electrodes maintained at –150 and +300 mV, respectively, was used for detection. Amino acids were analyzed using pre-column derivatization at 4°C and fluorescence detection. The derivatisation protocol was conducted by the autosampler as follows: 10 μL of 1 nM/μL homoserine (amino acid internal standard) was mixed with 10 μL of sample; then 20 μL of borate buffer (0.4 M at pH 10) was added and mixed; then 5 μL of OPA reagent (100 mg ophthalaldehyde in 1 ml methanol with 9 ml borate buffer and 50 μl mercaptoethanol) was added and mixed; then after a 30 sec wait, 50 μL of mobile phase was added and mixed; 5 μl of the final solution was injected into the HPLC system. The system consisted of an isocratic pump and autosampler (Dionex UltiMate 3000, Thermo Scientific), and fluorescence detector (Model 2475, Waters Corporation) equipped with a Phenomenex Gemini C18 column (4.6 mm × 150 mm, 3 um; Phenomenex, CA, USA). The mobile phase consisted of 0.05 M sodium acetate, tetrahydrofuran and acetonitrile (74:1:25, v/v) adjusted to pH 4.0 using 100% acetic acid. Flow rate was 1 ml/min and the fluorescence detector was set to an excitation wavelength of 337 nm and an emission wavelength of 454 nm. All data was stored and processed with Dionex Chromeleon software (version 7.2, Thermo Scientific). Data was quantified by calculating peak-area ratios of each compound compared to the relevant internal standard.

2.7. Gene expression array

The integrity of total RNAs was examined in an Agilent Bioanalyzer 2100 (Agilent Technologies, Santa Clara, CA, USA). Total RNA concentration was measured using the Nanodrop spectrophotometer. The mouse Agilent microarray service was performed by Phalanx Biotech (San Diego, CA). A total of 4 μg Cy5-labeled RNA targets were hybridized to Gene Expression v2 4×44K Microarrays (Agilent Technologies, Santa Clara, CA), according to the manufacturer's protocol. The data were analysed using the provided manufacturer's protocol. Following the hybridization, fluorescent signals were scanned using an Axon 4000 (Molecular Devices, Sunnyvale, CA, USA). Five replicates per condition were used. Microarray signal intensity of each spot was analysed using the GenePix 4.1 software (Molecular Devices, Sunnyvale, CA, USA). Each signal value was normalized using the R program in the limma linear models package (Bioconductor 3.2, https://bioconductor.org).

For the analysis of gene expression, raw data was loaded into ArrayStudio (Omicsoft Corporation, Cary, NC) and first filtered based on a built-in ANOVA, as well as a t-test, applied to fold changes between experimental and control conditions. Significant changes had a p value < 0.05. In addition, maximum least-squares (Max LS) mean ≥ 6, and a false discovery rate by the Benjamini-Hochberg correction (FDR_BH) <0.01 were applied. Using this method, many genes were found with raw p-values < 0.05, but if the FDR_BH did not reach < 0.01, they were discarded. In this particular analysis set, the genes were further filtered to express a robust above or below 3-fold significant, above background, gene expression change. The list of genes that were identified in the different groups following the described criteria, were loaded into Cytoscape 3.3 (http://cytoscape.org), using GeneMania (Warde-Farley et al., 2010), to identify significantly changed interaction networks of genes, and relevant pathways, particularly assigned to neuroactive ligand-receptor interactions in the Kyoto Encyclopedia of Genes and Genomes (KEGG) (www.genome.jp/kegg) and in Gene Ontology (GO) terms (http://geneontology.org/page/go-enrichment-analysis).

2.8. RT-PCR

RNA was reverse transcribed using SuperScript III Reverse Transcriptase (Invitrogen, Waltham, MA). Primers were purchased from Qiagen (Valencia, CA). PCRs were performed using RT² SYBR Green ROX FAST Mastermix (Qiagen), in a 7900HT Fast Real-Time PCR System with Fast 96-Well Block Module (Applied Biosystems, Foster City, CA) with a SDS Plate utility v2.2 software (Applied Biosystems). The results were normalized to the geometric mean of GAPDH and 18S housekeeping genes.

2.9. Immunohistochemistry

Following perfusion of the animal with ice-cold PBS, the brain tissue was harvested and fixed in 10% buffered formalin for 48 hrs, followed by 70% ethanol. Tissues were embedded in paraffin, cut into 5 μm sections, and mounted on glass slides. Rehydrated sections were blocked to endogenous peroxidase activity by treating slides with 3% hydrogen peroxide in absolute methanol. Following that, the slides were placed in a solution of 0.01M Citrate, pH 6.39, in a humidified heated chamber, for antigen exposure. Sections were blocked with 5g/l Casein (Sigma Aldrich) in PBS, containing 0.5g/l Thimerosal (Sigma Aldrich) and incubated with Iba-1 antibody (Wako Lab Chemicals, Richmond, VA), the anti-mouse DRD1 antibody (NLS43, Novus Biologicals, Littleton, CO), or anti mouse DRD2 (orb154598, Biorbyt, San Francisco, CA), each one diluted in Casein buffer. Biotinylated goat anti-rabbit IgG antibodies (Vector Labs, Burlingame, CA) were used at a 1/300 dilution. Visualization was achieved using biotin/avidin-peroxidase (Vector Labs) and Nova Red (Vector Labs). Counterstaining was made with Gill's hematoxylin. Images were captured using an Axiovert 200 inverted microscope (Carl Zeiss) with Axio Vision software (version 4.8.1; Carl Zeiss). Image analysis was performed in Fiji/ImageJ (NIH, USA). For that, tiff image files were opened and manually thresholded to identify stained cells. A binary mask was obtained from the negative thresholded image and measurement values were calculated as percentage of the total area. This was performed in a minimum of 5 fields per section, and two sections per animal. The results are expressed as normalized intensity density.

The DRD1 antibody was a rabbit polyclonal antibody against a Synthetic 15 amino acid peptide from the 3rd cytoplasmic domain of human DRD1, 94% conserved in mice. The DRD2 antibody was a rabbit polyclonal antibody against a synthetic 16 amino acid peptide from C-terminus cytoplasmic domain of human DRD2, conserved in both rats and mice. Both antibodies were positively validated in overexposed lysates by Western blot, and on cells that lack DRD1 and DRD2. Although validation was not performed in tissue-specific knockout mice, all the staining were performed in other tissues, including muscle, liver and spleen, that do not express or have small number of positive cells for these receptors.

2.10. Quantification of dopamine neuron recruitment

Mice were deeply anesthetized, then intracardially perfused with 50 mL phosphate buffer solution (PBS) followed by 50 mL 4% ice-cold PFA (10 mL/min). Brains were harvested and post-fixed overnight in 4% PFA at 4°C, then cryo-protected in 30% sucrose for 48 hours. Brains were snap frozen on dry ice and 30 μm sections were collected with a standard Leica Microtome (SM 2010R). Horizontal brain sections were collected through the VTA and substantia nigra compacta (SNc) for each mouse and stored in PBS for immediate use or in cryoprotectant for long-term storage at −20°C. VTA dopaminergic neurons were identified with standard 3,3′-diaminobenzidine (DAB) immunohistochemistry for tyrosine hydroxylase (TH). Section were washed 3 times for 10’ in PBS, then blocked in 5% horse normal serum/0.3% Triton in PBS for 1 hour before going in the primary antibody (mouse monoclonal anti-TH, 1:500, Millipore) solution overnight at 4°C. On the second day sections were washed for 3 times for 10’ in PBS then put in secondary antibody (biotinylated anti-mouse, 1:100, Vector) solution for 1 hour at room temperature. Following 3 PBS washes, sections were incubated in ABC solution (Vector) for 1 hour, washed again 3 times and incubated in fresh DAB solution for 2–4 minutes. After 3 final washes in PBS sections were counterstained with GIEMSA, then mounted in gelatin on glass slides, and coverslipped with Cytoseal mounting media (Thermo Scientific). Stained tissue was imaged with a slide scanner (Leica Aperio Nanozoomer). Stereological quantification of TH+ neurons in the SNc and VTA subnuclei, PN and PBP, was performed blind with the Stereologer software (Stereology Resource Center, Inc).

2.11. Statistical analyses

All of the analyses were performed with IBM SPSS Statistics 20 (Armonk, NY, USA). Data were analyzed using analysis of variance (ANOVA), with *TAT, Methamphetamine Exposure* (during acquisition), *Methamphetamine Challenge* or *Group* as the between-subject factors. Repeated-measures ANOVAs were used when additional within-subject factors were present (i.e., *Bin* or *Day*). TH+ cell counting data was analyzed non-parametrically using the Jonckheere-Terpstra Test for ordered alternatives. The *a priori* hypothesis was that methamphetamine exposure alone would have a larger effect on TH+ neuron recruitment compared with TAT expression, but the combination of both would result in the largest magnitude of change. When appropriate, *post hoc* comparisons were performed using Least Significant Difference (LSD) analyses. Results are expressed as mean ± SEM. Differences were considered statistically significant at $p < 0.05$.

3. Results

3.1. Methamphetamine-induced locomotor sensitization

There were significant main effects of *Day* ($F_{6,468}$=17.5, p<0.001) and *Methamphetamine Exposure* ($F_{1,78}$=207.8, p<0.001), and a significant interaction of *Day* × *Methamphetamine Exposure* ($F_{6,468}$=29.3, p<0.001) on locomotor activity. Methamphetamine increased the distance travelled compared with saline on all days of testing (p<0.001; Figure 1). The distance travelled in response to repeated methamphetamine injections also increased across Days 1–3, whereas the response to saline remained consistent across all days of testing. No differences between TAT− and TAT+ mice were observed (Figure 1).

The response to saline and methamphetamine challenge on day 15 were analyzed separately as a repeated measure of 10 three-minute time bins with *TAT* and *Methamphetamine Exposure* as the between subject factors. For the saline challenge (Figure 2A), there were significant main effects of *Bin* ($F_{9,243}$=73.6, p<0.001) and *Methamphetamine Exposure* ($F_{1,27}$=14.1, p<0.001) on distance travelled. Methamphetamine exposure during the acquisition phase increased the locomotor response to saline challenge across all time points compared with prior saline exposure.

For the methamphetamine challenge (Figure 2B), there were significant main effects of *Bin* ($F_{9,423}$=8.1, p<0.001), *Methamphetamine Exposure* ($F_{1,47}$=113.9, p<0.001), *TAT* ($F_{1,47}$=7.5, p<0.01), and a significant interaction of *Bin* × *Methamphetamine Exposure* ($F_{9,423}$=12.2, p<0.001). Methamphetamine exposure significantly increased the locomotor response to methamphetamine challenge in all mice. Overall, TAT+ mice showed higher locomotor activity than TAT− mice with the largest difference between genotypes after methamphetamine exposure (p<0.01).

3.2. Dopamine expression profiles and IBA-1 expression in the caudate putamen

Using an Agilent mouse gene expression platform, we identified signature genes that characterize TAT expression, methamphetamine exposure during the acquisition phase, and their interaction in the CPu of mice challenged with methamphetamine. Interestingly, methamphetamine, compared with saline, caused a remarkable segregation of gene expression patterns in TAT− mice, affecting 8.6% of all the genes. TAT expression in saline-exposed mice had a limited effect on gene expression, by affecting only 0.07% of all the genes. However, in methamphetamine-exposed mice, TAT expression affected over 10% of the genes analysed. This was confirmed by predictions using General Linear model.

A substantial number of gene signatures overlapped with anti-correlated interactions, when methamphetamine exposure was compared to saline exposure in TAT− mice, and when methamphetamine exposure in TAT+ mice was compared to methamphetamine exposure in TAT− mice. We identified patterns that distinguished the groups, by focusing on genes in the dopamine system. We detected a significant effect of TAT on the expression of DRDs, and molecules associated with the dopamine system pathway. Figure 3 shows the graphical representation of these comparisons, as determined by a systems analysis using GeneMania *Mus musculus* network, excluding predicted interactions, in the Cytoscape platform. The examination of the effects of TAT expression (TAT+ vs. TAT− after exposure to saline;

Figure 3A) showed a significant downregulation of DRD4, Intersectin 1 (Itsn1) and Peptidylglycine Alpha-Amidating Monooxygenase (Pam), while genes such as the Gamma-Aminobutyric Acid Type A Receptor Theta Subunit (Gabrq) were upregulated. Similarly, methamphetamine exposure compared to saline exposure in TAT− mice; Figure 3B) caused a decrease of the expression of DRD4 and Pam, and also decreased DRD1a, DRD2, DRD3, regulatory molecules ADORA1 and ADORA2B, as well as epsilon (ε)-sarcoglycan (Sgce), Regulator Of G-Protein Signalling 20 (Rgs20), Ubiquitin C-Terminal Hydrolase L1 (Uchl1), NADH-ubiquinone oxidoreductase complex (complex I) of the mitochondrial respiratory (Ndufv2), and Monooxygenase, DBH-Like 2 (Moxd2). The effects of methamphetamine exposure in the context of TAT expression (methamphetamine vs saline exposure in TAT+ mice; Figure 3C) showed a modest effect in the dopamine system, although a trend for downregulation was maintained. In this case, though, methamphetamine exposure in TAT+ mice caused a significant increase in Pam levels and a significant decrease in Tata-box binding peptide (Tbp) levels. The effects of TAT expression in the context of methamphetamine exposure (TAT+ vs. TAT− mice exposed to methamphetamine; Figure 3D) increased DRD4, ADORA1 and ADORA2b, as well as Ndufv2, Cdnf and Uchl1.

In addition, we performed IHC analyses to estimate changes of intensity and distribution of the molecules of DRD1 and DRD2 at the protein level in the CPu (Figure 4). For DRD1, there was a significant main effect of *TAT* ($F_{3,16}$=107.1, p<0.0001). TAT+ mice had a significantly lower intensity density of DRD1 protein expression than TAT− mice independent of methamphetamine exposure. For DRD2, there were significant main effects of *TAT* ($F_{3,16}$=56.5, p<0.0001), *Methamphetamine exposure* ($F_{3,16}$=13.2, p<0.01) and their interaction ($F_{3,16}$=9.9, p<0.01). TAT+ SAL group had a significantly lower intensity density of DRD2 protein expression than TAT− SAL group (p<0.01); while TAT+ METH+ group had a significantly lower intensity density of DRD2 protein expression compared to all other groups (p<0.001).

We also examined whether TAT and/or methamphetamine had an effect on IBA-1, a marker for microglia activation (Figure 4). For IBA-1 intensity density, there were significant main effects of *TAT* ($F_{3,16}$=7.7, p<0.05), *Methamphetamine exposure* ($F_{3,16}$=28.1, p<0.001) but no interaction. A step-wise increase in the IBA-1 intensity density between the groups was observed, with the TAT− SAL group showing the lowest IBA-1 intensity density followed by the TAT+ SAL group and the TAT− METH group, with the greatest IBA-1 intensity density in the TAT+ METH group (linear trend analyses: slope 0.000665, R^2=0.75, p<0.0001).

3.3. Nucleus accumbens neurochemistry, dopamine and adenosine receptors expression

Levels of norepinephrine, dopamine, serotonin, glutamate, GABA, and associated metabolites, in the Acb were not significantly different between TAT− and TAT+ mice, regardless of methamphetamine exposure or challenge (Table 1 and Table 2).

In mice challenged with methamphetamine, there were significant main effects of *TAT* for the levels of all DRDs: DRD1 ($F_{1,16}$=9.3, p<0.01), DRD2 ($F_{1,16}$=35.6, p<0.001), DRD4 ($F_{1,16}$=9.3, p<0.01) and DRD5 ($F_{1,16}$=7.9, p<0.05). In addition, TAT+ mice had decreased levels of all the DRDs compared with TAT− mice, regardless of methamphetamine exposure

(Figure 5A). There were no differences between groups in the intensity density for DRD1 and DRD2 in the Acb (data not shown).

For the ADORAs, there were significant main effects of *TAT* for ADORA2A ($F_{1,16}$=16.6, p<0.001) and of *Methamphetamine Exposure* for ADORA1 ($F_{1,16}$=8.6, p<0.01), ADORA2A ($F_{1,16}$=5.8, p<0.05) and ADORA2B ($F_{1,16}$=7.4, p<0.05). TAT+ mice had significantly increased ADORA2A receptor levels compared with TAT− mice, regardless of methamphetamine exposure (Figure 5B). Methamphetamine exposure decreased the levels of all ADORA compared with saline exposure. There was also a significant interaction of *Methamphetamine Exposure* × *TAT* for the ADORA1 receptor ($F_{1,16}$=12.8, p<0.01). Methamphetamine exposure significantly lowered levels of the ADORA1 receptor in TAT- mice compared with saline treatment (p<0.001) but did not in TAT+ mice (Figure 5B).

3.4. Quantification of Dopaminergic neurons

We examined whether TAT and/or methamphetamine had an effect on the recruiting of a newly expressing dopaminergic neuronal pool. For that, TH+ neurons were detected in dopaminergic nuclei of the ventral tegmental area (VTA) and substantia nigra pars compacta (SNc) by immunohistochemistry using the colorimetric DAB amplification system (Figure 6A). The number of TH+ neurons (Figure 6D) were significantly different between groups in the parabrachial pigmented region (PBP, Figure 6B–C) of the VTA (T_{JT}=2.9, p<0.01). Methamphetamine exposure increased the number of TH+ neurons in both TAT− (p<0.05) and TAT+ (p<0.05) mice compared with TAT− SAL/METH mice. A step-wise increase in the number of TH+ cells between the groups was observed, with the TAT− SAL/METH group showing the lowest number followed by the TAT+ SAL/METH group and the TAT- METH/METH group, with the greatest level number of TH+ cells in the TAT+ METH/ METH group.

4. Discussion

The present studies demonstrate that brain-specific TAT expression during methamphetamine exposure augments methamphetamine-induced locomotor sensitization. TAT expression, regardless of methamphetamine sensitization, decreases striatal DRD and ADORA expression. The combination of TAT expression and methamphetamine sensitization was associated with increased expression of ADORAs (specifically, ADORA1A) and induction of neurotransmitter plasticity (Dulcis and Spitzer 2008, 2012; Dulcis et al. 2013) measured as an increased number of dopamine neurons in the parabrachial pigmented region of the VTA. These results demonstrate that combined TAT expression and methamphetamine exposure alter dopamine signaling and enhance the recruitment of reserve pool neurons of non-dopaminergic neurons to a dopamine phenotype. Previous evidence of increased sensitivity to methamphetamine reward (Kesby et al. 2016b), which occurs in addition to methamphetamine-induced increase in activity, suggests that HIV-positive subjects may be more susceptible to the effects of methamphetamine compared to HIV-negative subjects. Finally, TAT expression and methamphetamine exposure significantly increased microglia activation indicative of increased inflammatory processes with the largest effect after combined exposure.

TAT expression has been shown to increase the rewarding effects of methamphetamine (Kesby et al. 2016b), ethanol (McLaughlin et al. 2015) and cocaine (Paris et al. 2014c). However, the effects of TAT exposure on psychostimulant-induced locomotor sensitization are mixed. For example, TAT−expressing mice and rats with intra-Acb TAT injections show an increased locomotor response to acute cocaine (Harrod et al. 2008; Paris et al. 2014c). However, intra-Acb injections of TAT before or after acquisition of cocaine sensitization have been shown to decrease sensitized locomotor responses (Ferris et al. 2010; Harrod et al. 2008). Similarly, intra-VTA TAT injections attenuate nicotine sensitization in rats (Zhu et al. 2015). However, it is not known whether acute local injections of the TAT protein are comparable to the prolonged TAT expression of TAT-expressing mouse model utilized in our study (Paris et al. 2014b). Importantly, locomotor response to repeated methamphetamine injections was similar in TAT+ and TAT− mice indicating similar sensitivity to methamphetamine during the acquisition phase. Thus, our data suggests that the period of abstinence prior to challenge is critical to reveal increased sensitivity to methamphetamine-induced sensitization in TAT+ mice.

In a rat model of amphetamine sensitization, increases in c-Fos reactive cells were observed in a direct target of the VTA, the Acb (Nordquist et al. 2008), suggesting a functional link between increased activity of dopamine neurons, which are recruited in response to amphetamine after sensitization, and the Acb. Our results are the first example, to the best of our knowledge, of neurotransmitter plasticity associated with methamphetamine sensitization eliciting an increase in the number of newly expressing dopamine neurons. Because a greater number of dopamine neurons was observed following TAT expression and methamphetamine sensitization, a potential neuroadaptive response to chronic psychostimulant exposure might occur in HIV infection. The recruitment of dopaminergic neurons was specific to the parabrachial pigmented region of the VTA while SNc was unaltered, consistent with the existence of dopamine projections from this region to the Acb (Lammel et al. 2014) and a key role in the induced locomotion (Heusner et al. 2003). In our previous studies (Dulcis and Spitzer 2008; Dulcis et al. 2013), we found that neurotransmitter plasticity is regulated at the transcriptional level and that newly-expressing dopaminergic neurons start expressing *de novo* TH transcripts following induction. Understanding the mechanism of gene regulation behind methamphetamine-induced dopamine plasticity in TAT+ mice is an important question that we would like to address in the near future. Our behavioral and functional findings associated with changes in the number of dopaminergic neurons in the VTA could result from either transcriptional or translational regulation that ultimately would increase dopamine expression and release in the Acb. However, although we found evidence of a greater population of dopamine neurons in the VTA, we did not observe alterations in dopamine levels or turnover within the Acb. This result is not surprising because the effects of TAT expression on dopamine levels are time-dependent. That is, in our previous work, TAT expression does alter dopamine and serotonin levels three days after the final doxycycline treatment (Kesby et al. 2016b), but this effect dissipated by later time points with monoamine levels similar in TAT+ and TAT− mice (Kesby et al. 2016b; Kesby et al. 2016c). Therefore, the availability of more dopamine neurons alongside parallel changes in receptor expression, would appear sufficient to explain the augmented sensitization behavior observed in TAT+ mice.

A complex relationship between TAT expression and methamphetamine exposure was revealed by the differential impact of these factors on receptor expression. The expression of molecules associated with the dopaminergic system, such as the DRDs and the ADORAs, was particularly affected both by TAT and methamphetamine, combined or alone, In both the Acb and CPu, induction of TAT expression tended to downregulate DRD mRNA and protein levels when compared with similarly treated TAT− mice, suggesting a general effect on dopamine neurons. However, some discrepancies between gene expression and protein expression for DRDs were also observed. For example, after methamphetamine exposure we observed increased DRD mRNA expression in the CPu of TAT+ compared with TAT− mice, whereas, DRD2 protein expression was decreased. Multiple factors could contribute to differential mRNA and protein expression outcomes, such as the half-life of proteins and mRNA degradation rates, the lower rate of mRNA transcription compared to protein translation in mammalian cells (Vogel and Marcotte 2012). An additional contributing factor to consider is the acute effects of methamphetamine challenge (likely observed in mRNA expression) versus chronic effects of methamphetamine exposure during acquisition and TAT induction phases (likely observed in protein levels). Nevertheless, these data suggest that dopamine systems are profoundly affected by both methamphetamine and TAT exposure.

Both the Acb and CPu are heavily involved in the transition to drug dependence (Everitt and Robbins 2013). Adaptations in the CPu has been associated with methamphetamine sensitization (Li et al. 2016a; Li et al. 2016b; Yan et al. 2014). However, the subdivisions of the striatum have important functional differences that need to be considered (Boekhoudt et al. 2016). Indeed, we have previously shown that the effects of FTAT expression on dopamine levels in the CPu and Acb are opposing in nature (Kesby et al. 2016b). Further, our results suggest a differential recruitment of TH+ cells in parabrachial pigmented region of the VTA, but not the SN, which may instead support differential effects on striatonigral and mesolimbic dopamine circuitry.

Similar to DRDs, increased ADORA receptor expression both in the CPu and Acb was observed in TAT+ mice exposed to methamphetamine compared to TAT-mice. In the Acb, ADORA1 receptor levels were significantly increased in methamphetamine sensitized TAT+ mice compared with methamphetamine sensitized TAT− mice. In addition, regardless of methamphetamine exposure, TAT expression also led to increased levels of ADORA2A. A complex balance between ADORA1 and ADORA2A receptors is required for functional dopaminergic signaling. For example, ADORA1 receptors inhibit whereas, ADORA2A receptors stimulate dopamine and glutamate release in the Acb (Quarta et al. 2004). In addition, stimulation of ADORA1 receptors negatively affects DRD1 binding, while stimulation of ADORA2A receptors decreases the affinity for DRD2 (Franco et al. 2000). The differential feedback pathways involving striatal DRD1 and DRD2-bearing neurons in locomotion are also complex (Calabresi et al. 2014). Thus, the control of psychostimulant-induced locomotion involves the contribution of multiple factors including dopamine neuron function and a balance between DRD1 and DRD2 pathways. The combination of TAT expression and methamphetamine sensitization may likely disrupt such balance.

The systems analysis was instrumental in identifying other potential genes contributing to the enhanced sensitivity to methamphetamine in TAT+ mice. For example, the Peptidylglycine Alpha-Amidating Monooxygenase (Pam) gene, which was independently downregulated by methamphetamine exposure or by TAT expression, was upregulated by the combined methamphetamine exposure in the context of TAT expression. Pam is an essential cuproenzyme and regulator of copper homeostasis in neuroendocrine cells. More recently, Pam has been identified as a possible cellular oxygen sensor (Simpson et al. 2015) suggesting our observations may be in response to oxidative stress or hypoxia induced by TAT, methamphetamine or a combination of the two. Both methamphetamine exposure and TAT expression are associated with oxidative stress (Krasnova and Cadet 2009; Mediouni et al. 2015). Multiple other genes, including Ndufv2 (NADH dehydrogenase [ubiquinone] flavoprotein 2), Cdnf (Conserved dopamine neurotrophic factor) and Uchl1 (ubiquitin C-terminal hydrolase-L1), were also upregulated in sensitized TAT+ mice compared with sensitized TAT− mice. These genes are strongly associated with dopaminergic systems and oxidative stress. For example, Ndufv2 is a mitochondrial protein associated with oxidative stress, aging and a range of neuropsychiatric disorders (Tatarkova et al. 2016). Cdnf is an neurotrophic factor that promotes the survival of midbrain dopaminergic neurons (Lindahl et al. 2016). Therefore, upregulation of Cdnf in methamphetamine-sensitized TAT+ mice compared with methamphetamine-sensitized TAT− mice may be in response to increased levels of oxidative stress, and it may be compatible with our observation of increases in the reserve pool neuron recruitment to a dopaminergic phenotype. Uchl1 is important in the removal of oxidized/damaged proteins and decreases are associated with neurodegenerative disorders (Tramutola et al. 2016). Thus, upregulation of this gene in sensitized TAT+ mice compared with TAT− mice could be a result of increased levels of oxidized/damaged proteins or alternatively, of oxidative damage to Uchl1 itself, which can lead to functional impairment (Tramutola et al. 2016). Indeed, higher levels of Uchl1 after traumatic brain injury are associated with worse outcomes (Takala et al. 2016). The genetic changes observed in the present study are indicative of neuronal damage. Cerebral microgliosis, suggesting neuronal damage, has been reported in humans with HIV and life-time methamphetamine abuse (Soontornniyomkij et al. 2016). In our model, we have identified evidence of glial activation as demonstrated by increased IBA-1 expression in the CPu, particularly in the methamphetamine-exposed groups, which was further enhanced by TAT expression. The changes in these genes caused by TAT protein and methamphetamine exposure further highlight the importance of TAT expression in the brain, in the context of drug sensitization, on a network of genes regulating the dopaminergic system and reward function.

5. Conclusions

We present experimental evidence that the combination of HIV-related protein TAT and methamphetamine exposure affects molecular pathways that may lead to altered reward and cognitive function in HIV+ individuals with methamphetamine abuse. Our work demonstrates that the HIV-associated TAT protein augments the neurobiological adaptations underpinning sensitization to methamphetamine in mice. These adaptations include increases in the number of VTA dopamine neurons, altered expression of DRDs and

ADORAs, and dysregulation of a network of genes associated with both the dopamine system and oxidative stress. The transient expression of the TAT protein also suggests that these adaptations persist in the absence of the TAT protein. Further studies on the role of ADORAs and on the contribution of newly expressing dopamine neurons, in the context of HIV and methamphetamine, may shed light on potential therapeutic targets for comorbid methamphetamine abuse in HIV+ individuals.

Acknowledgments

This work was supported by the Translational Methamphetamine AIDS Research Center funded by the National Institute on Drug Abuse (TMARC P50 DA26306), a National Institute on Drug Abuse grants (DA033849 to SS, DA036164 to MCGM), the W.M. Keck Foundation Award (855F9A to DD), the Clinical and Translational Research Institute UC San Diego grant (UL1TR001442 to AB), and the Interdisciplinary Research Fellowship in NeuroAIDS (IRFN fellowship to JPK, MH081482).

References

Boekhoudt L, Omrani A, Luijendijk MC, Wolterink-Donselaar IG, Wijbrans EC, van der Plasse G, Adan RA. Chemogenetic activation of dopamine neurons in the ventral tegmental area, but not substantia nigra, induces hyperactivity in rats. Eur Neuropsychopharmacol. 2016; 26:1784–1793. [PubMed: 27712862]

Calabresi P, Picconi B, Tozzi A, Ghiglieri V, Di Filippo M. Direct and indirect pathways of basal ganglia: a critical reappraisal. Nature Neuroscience. 2014; 17:1022–1030. [PubMed: 25065439]

Carey AN, Sypek EI, Singh HD, Kaufman MJ, McLaughlin JP. Expression of HIV-Tat protein is associated with learning and memory deficits in the mouse. Behav Brain Res. 2012; 229:48–56. [PubMed: 22197678]

Chesworth R, Brown RM, Kim JH, Ledent C, Lawrence AJ. Adenosine 2A receptors modulate reward behaviours for methamphetamine. Addict Biol. 2016; 21:407–421. [PubMed: 25612195]

Dulcis D, Spitzer NC. Illumination controls differentiation of dopamine neurons regulating behaviour. Nature. 2008; 456:195–201. [PubMed: 19005547]

Dulcis D, Spitzer NC. Reserve pool neuron transmitter respecification: Novel neuroplasticity. Dev Neurobiol. 2012; 72:465–474. [PubMed: 21595049]

Dulcis D, Jamshidi P, Leutgeb S, Spitzer NC. Neurotransmitter switching in the adult brain regulates behavior. Science. 2013; 340:449–453. [PubMed: 23620046]

Everitt BJ, Robbins TW. From the ventral to the dorsal striatum: devolving views of their roles in drug addiction. Neurosci Biobehav Rev. 2013; 37:1946–1954. [PubMed: 23438892]

Ferre S, Fredholm BB, Morelli M, Popoli P, Fuxe K. Adenosine-dopamine r eceptor-receptor interactions as an integrative mechanism in the basal ganglia. Trends Neurosci. 1997; 20:482–487. [PubMed: 9347617]

Ferris MJ, Mactutus CF, Booze RM. Neurotoxic profiles of HIV, psychostimulant drugs of abuse, and their concerted effect on the brain: current status of dopamine system vulnerability in NeuroAIDS. Neurosci Biobehav Rev. 2008; 32:883–909. [PubMed: 18430470]

Ferris MJ, Frederick-Duus D, Fadel J, Mactutus CF, Booze RM. In vivo microdialysis in awake, freely moving rats demonstrates HIV-1 Tat-induced alterations in dopamine transmission. Synapse. 2009; 63:181–185. [PubMed: 19086089]

Ferris MJ, Frederick-Duus D, Fadel J, Mactutus CF, Booze RM. Hyperdopaminergic tone in HIV-1 protein treated rats and cocaine sensitization. Journal of Neurochemistry. 2010; 115:885–896. [PubMed: 20796175]

Franco R, et al. Evidence for adenosine/dopamine receptor interactions: indications for heteromerization. Neuropsychopharmacology. 2000; 23:S50–59. [PubMed: 11008067]

Groves NJ, Kesby JP, Eyles DW, McGrath JJ, Mackay-Sim A, Burne THJ. Adult vitamin D deficiency leads to behavioural and brain neurochemical alterations in C57BL/6J and BALB/c mice. Behav Brain Res. 2013; 241:120–131. [PubMed: 23238039]

Harrod SB, Mactutus CF, Fitting S, Hasselrot U, Booze RM. Intra-accumbal Tat(1–72) alters acute and sensitized responses to cocaine. Pharmacol Biochem Behav. 2008; 90:723–729. [PubMed: 18582493]

Heusner CL, Hnasko TS, Szczypka MS, Liu Y, During MJ, Palmiter RD. Viral restoration of dopamine to the nucleus accumbens is sufficient to induce a locomotor response to amphetamine. Brain Research. 2003; 980:266–274. [PubMed: 12867267]

Jing L, Zhang M, Li JX, Huang P, Liu Q, Li YL, Liang H, Liang JH. Comparison of single versus repeated methamphetamine injection induced behavioral sensitization in mice. Neurosci Lett. 2014; 560:103–106. [PubMed: 24361545]

Kavanagh KA, Schreiner DC, Levis SC, O'Neill CE, Bachtell RK. Role of adenosine receptor subtypes in methamphetamine reward and reinforcement. Neuropharmacology. 2015; 89:265–273. [PubMed: 25301277]

Kesby JP, Markou A, Semenova S. The effects of HIV-1 regulatory TAT protein expression on brain reward function, response to psychostimulants and delay-dependent memory in mice. Neuropharmacology. 2016a; 109:205–215. doi:http://dx.doi.org/10.1016/j.neuropharm.2016.06.011. [PubMed: 27316905]

Kesby JP, Markou A, Semenova S. The effects of HIV-1 regulatory TAT protein expression on brain reward function, response to psychostimulants and delay-dependent memory in mice. Neuropharmacology. 2016b; 109:205–215. [PubMed: 27316905]

Kesby JP, Markou A, Semenova S. Effects of HIV/TAT protein expression and chronic selegiline treatment on spatial memory, reversal learning and neurotransmitter levels in mice. Behav Brain Res. 2016c; 311:131–140. doi:http://dx.doi.org/10.1016/j.bbr.2016.05.034. [PubMed: 27211061]

Kesby JP, Hubbard DT, Markou A, Semenova S. Expression of HIV gp120 protein increases sensitivity to the rewarding properties of methamphetamine in mice. Addict Biol. 2014; 19:593–605. [PubMed: 23252824]

Kesby JP, Cui X, Ko P, McGrath JJ, Burne TH, Eyles DW. Developmental vitamin D deficiency alters dopamine turnover in neonatal rat forebrain. Neurosci Lett. 2009; 461:155–158. [PubMed: 19500655]

Kim BO, Liu Y, Ruan YW, Xu ZC, Schantz L, He JJ. Neuropathologies in transgenic mice expressing human immunodeficiency virus type 1 tat protein under the regulation of the astrocyte-specific glial fibrillary acidic protein promoter and doxycycline. American Journal of Pathology. 2003; 162:1693–1707. [PubMed: 12707054]

Koob GF, Volkow ND. Neurocircuitry of addiction. Neuropsychopharmacology. 2010; 35:217–238. [PubMed: 19710631]

Krasnova IN, Cadet JL. Methamphetamine toxicity and messengers of death. Brain Research Reviews. 2009; 60:379–407. [PubMed: 19328213]

Kumar AM, Ownby RL, Waldrop-Valverde D, Fernandez B, Kumar M. Human immunodeficiency virus infection in the CNS and decreased dopamine availability: relationship with neuropsychological performance. J Neurovirol. 2011; 17:26–40. [PubMed: 21165787]

Lammel S, Lim BK, Malenka RC. Reward and aversion in a heterogeneous midbrain dopamine system. Neuropharmacology. 2014; 76(Pt B):351–359. [PubMed: 23578393]

Lewis BB, Miller LE, Herbst WA, Saha MS. The role of voltage-gated calcium channels in neurotransmitter phenotype specification: Coexpression and functional analysis in Xenopus laevis. Journal of Comparative Neurology. 2014; 522:2518–2531. [PubMed: 24477801]

Li L, Liu X, Qiao C, Chen G, Li T. Ifenprodil Attenuates Methamphetamine-Induced Behavioral Sensitization and Activation of Ras-ERK-FosB Pathway in the Caudate Putamen. Neurochem Res. 2016a; 41:2636–2644. [PubMed: 27339870]

Li L, Qiao C, Chen G, Qian H, Hou Y, Li T, Liu X. Ifenprodil attenuates the acquisition and expression of methamphetamine-induced behavioral sensitization and activation of Ras-ERK1/2 cascade in the caudate putamen. Neuroscience. 2016b; 335:20–29. [PubMed: 27544406]

Lindahl M, Saarma M, Lindholm P. Unconventional neurotrophic factors CDNF and MANF: structure, physiological functions and therapeutic potential. Neurobiol Dis. 2016

McLaughlin JP, Ganno ML, Eans SO, Mizrachi E, Paris JJ. HIV-1 Tat Protein Exposure Potentiates Ethanol Reward and Reinstates Extinguished Ethanol-Conditioned Place Preference. Curr Hiv Res. 2015; 12:415–423.

Mediouni S, Marcondes MCG, Miller C, McLaughlin JP, Valente ST. The cross-talk of HIV-1 Tat and methamphetamine in HIV-associated neurocognitive disorders. Front Microbiol. 2015; 6:24. [PubMed: 25688238]

Mediouni S, et al. Antiretroviral therapy does not block the secretion of the human immunodeficiency virus tat protein. Infect Disord Drug Targets. 2012; 12:81–86. [PubMed: 22280310]

Merino JJ, et al. HIV-1 neuropathogenesis: therapeutic strategies against neuronal loss induced by gp120/Tat glycoprotein in the central nervous system. Revista De Neurologia. 2011; 52:101–111. [PubMed: 21271550]

Midde NM, Gomez AM, Zhu J. HIV-1 Tat Protein Decreases Dopamine Transporter Cell Surface Expression and Vesicular Monoamine Transporter-2 Function in Rat Striatal Synaptosomes. J Neuroimmune Pharm. 2012; 7:629–639.

Nagarajan R, et al. Neuropsychological Function and Cerebral Metabolites in HIV-infected Youth. J Neuroimmune Pharm. 2012; 7:981–990.

Nelson SB, Turrigiano GG. Strength through diversity. Neuron. 2008; 60:477–482. [PubMed: 18995822]

Nordquist RE, Vanderschuren LJ, Jonker AJ, Bergsma M, de Vries TJ, Pennartz CM, Voorn P. Expression of amphetamine sensitization is associated with recruitment of a reactive neuronal population in the nucleus accumbens core. Psychopharmacology (Berl). 2008; 198:113–126. [PubMed: 18347780]

Paris JJ, Singh HD, Ganno ML, Jackson P, McLaughlin JP. Anxiety-like behavior of mice produced by conditional central expression of the HIV-1 regulatory protein, Tat. Psychopharmacology (Berl). 2014a; 231:2349–2360. [PubMed: 24352568]

Paris JJ, Singh HD, Ganno ML, Jackson P, McLaughlin JP. Anxiety-like behavior of mice produced by conditional central expression of the HIV-1 regulatory protein, Tat. Psychopharmacology. 2014b; 231:2349–2360. [PubMed: 24352568]

Paris JJ, Carey AN, Shay CF, Gomes SM, He JJ, McLaughlin JP. Effects of Conditional Central Expression of HIV-1 Tat Protein to Potentiate Cocaine-Mediated Psychostimulation and Reward Among Male Mice. Neuropsychopharmacology. 2014c; 39:380–388. [PubMed: 23945478]

Pierce RC, Kalivas PW. A circuitry model of the expression of behavioral sensitization to amphetamine-like psychostimulants. Brain Res Brain Res Rev. 1997; 25:192–216. [PubMed: 9403138]

Purohit V, Rapaka R, Shurtleff D. Drugs of Abuse, Dopamine, and HIV-Associated Neurocognitive Disorders/HIV-Associated Dementia. Mol Neurobiol. 2011; 44:102–110. [PubMed: 21717292]

Quarta D, et al. Adenosine receptor-mediated modulation of dopamine release in the nucleus accumbens depends on glutamate neurotransmission and N-methyl-D-aspartate receptor stimulation. Journal of Neurochemistry. 2004; 91:873–880. [PubMed: 15525341]

Rajasingham R, Mimiaga MJ, White JM, Pinkston MM, Baden RP, Mitty JA. A systematic review of behavioral and treatment outcome studies among HIV-infected men who have sex with men who abuse crystal methamphetamine. AIDS Patient Care STDS. 2012; 26:36–52. [PubMed: 22070609]

Robinson TE, Berridge KC. Review. The incentive sensitization theory of addiction: some current issues. Philos Trans R Soc Lond B Biol Sci. 2008

Shimazoe T, Yoshimatsu A, Kawashimo A, Watanabe S. Roles of adenosine A(1) and A(2A) receptors in the expression and development of methamphetamine-induced sensitization. Eur J Pharmacol. 2000; 388:249–254. [PubMed: 10675733]

Shoptaw S, Peck J, Reback CJ, Rotheram-Fuller E. Psychiatric and substance dependence comorbidities, sexually transmitted diseases, and risk behaviors among methamphetamine-dependent gay and bisexual men seeking outpatient drug abuse treatment. J Psychoactive Drugs. 2003; 35(Suppl 1):161–168. [PubMed: 12825759]

Simpson PD, Eipper BA, Katz MJ, Gandara L, Wappner P, Fischer R, Hodson EJ, Ratcliffe PJ, Masson N. Striking Oxygen Sensitivity of the Peptidylglycine alpha-Amidating Monooxygenase (PAM) in Neuroendocrine Cells. J Biol Chem. 2015; 290:24891–24901. [PubMed: 26296884]

Soontornniyomkij V, Umlauf A, Soontornniyomkij B, Batki IB, Moore DJ, Masliah E, Achim CL. Lifetime methamphetamine dependence is associated with cerebral microgliosis in HIV-1-infected adults. J Neurovirol. 2016; 22:650–660. [PubMed: 27098516]

Steketee JD. Neurotransmitter systems of the medial prefrontal cortex: potential role in sensitization to psychostimulants. Brain Res Brain Res Rev. 2003; 41:203–228. [PubMed: 12663081]

Takala RS, et al. Glial Fibrillary Acidic Protein and Ubiquitin C-Terminal Hydrolase-L1 as Outcome Predictors in Traumatic Brain Injury. World Neurosurg. 2016; 87:8–20. [PubMed: 26547005]

Tatarkova Z, Kovalska M, Timkova V, Racay P, Lehotsky J, Kaplan P. The Effect of Aging on Mitochondrial Complex I and the Extent of Oxidative Stress in the Rat Brain Cortex. Neurochemical Research. 2016; 41:2160–2172. [PubMed: 27161369]

Theodore S, Cass WA, Dwoskin LP, Maragos WF. HIV-1 protein Tat inhibits vesicular monoamine transporter-2 activity in rat striatum. Synapse. 2012; 66:755–757. [PubMed: 22517264]

Tramutola A, Di Domenico F, Barone E, Perluigi M, Butterfield DA. It Is All about (U)biquitin: Role of Altered Ubiquitin-Proteasome System and UCHL1 in Alzheimer Disease. Oxid Med Cell Longev. 2016; 2016:2756068. [PubMed: 26881020]

Velazquez-Ulloa NA, Spitzer NC, Dulcis D. Contexts for dopamine specification by calcium spike activity in the CNS. J Neurosci. 2011; 31:78–88. [PubMed: 21209192]

Vogel C, Marcotte EM. Insights into the regulation of protein abundance from proteomic and transcriptomic analyses. Nat Rev Genet. 2012; 13:227–232. [PubMed: 22411467]

Yan T, Li L, Sun B, Liu F, Yang P, Chen T, Li T, Liu X. Luteolin inhibits behavioral sensitization by blocking methamphetamine-induced MAPK pathway activation in the caudate putamen in mice. PLoS One. 2014; 9:e98981. [PubMed: 24901319]

Zhu J, Mactutus CF, Wallace DR, Booze RM. HIV-1 Tat protein-induced rapid and reversible decrease in [3H]dopamine uptake: dissociation of [3H]dopamine uptake and [3H]2beta-carbomethoxy-3-beta-(4-fluorophenyl)tropane (WIN 35,428) binding in rat striatal synaptosomes. J Pharmacol Exp Ther. 2009; 329:1071–1083. [PubMed: 19325033]

Zhu J, Midde NM, Gomez AM, Sun WL, Harrod SB. Intra-ventral tegmental area HIV-1 Tat(1–86) attenuates nicotine-mediated locomotor sensitization and alters mesocorticolimbic ERK and CREB signaling in rats. Front Microbiol. 2015; 6:17. [PubMed: 25667586]

Highlights

- TAT expression in the brain enhances sensitivity to methamphetamine.
- TAT expression decreased striatal dopamine receptors expression.
- TAT expression and methamphetamine increased recruitment of midbrain dopamine neurons.
- TAT expression and methamphetamine differentially modulated adenosine receptors expression.
- TAT-induced neuroadaptations may contribute to comorbid methamphetamine abuse and HIV.

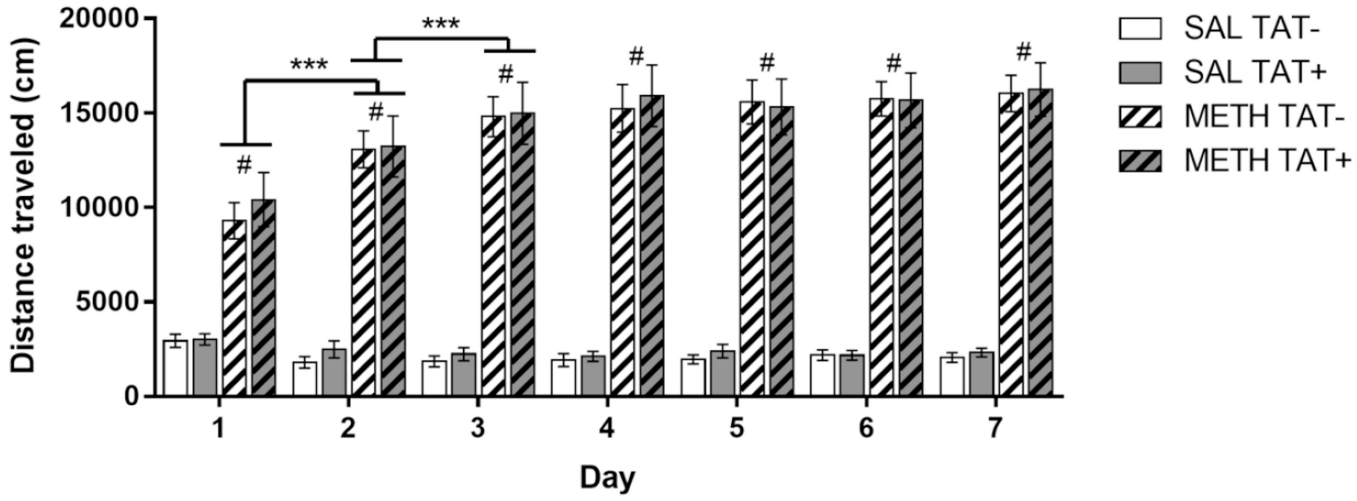

Figure 1. Effects of TAT protein expression on locomotor activity during repeated methamphetamine administration

Mice were treated daily with saline (SAL) or 2 mg/kg methamphetamine (METH; striped bars) and the total distance travelled (cm) over 30 min was assessed. Methamphetamine exposure significantly increased locomotor activity compared with saline at all days of testing. Methamphetamine-induced increases in locomotor activity were larger on Day 2 than Day 1, and on Day 3 compared to Day 2 ($P < 0.001$). No differences between TAT− and TAT+ mice were observed on the distance travelled after saline or methamphetamine. Data are expressed as Mean ± SEM (n=19–23). *** $p < 0.001$. $^{\#}$ $p < 0.001$ compared to saline treatment on the corresponding day of testing.

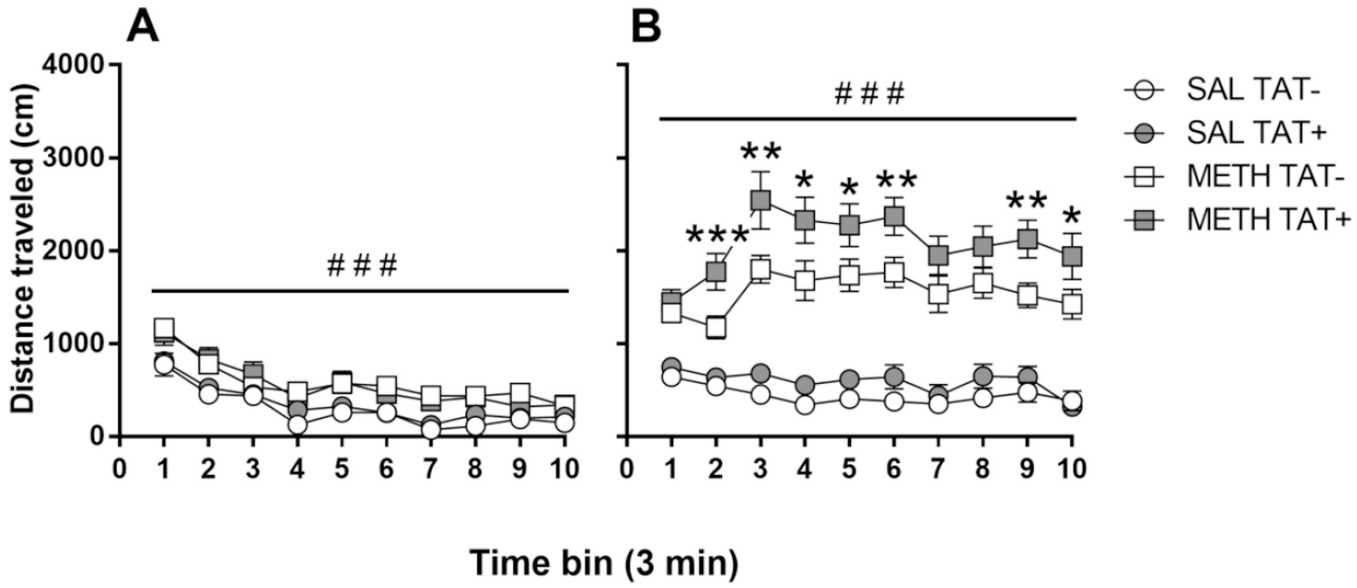

Figure 2. Effects of TAT protein expression and methamphetamine exposure on the sensitized locomotor response

Locomotor responses to challenge with saline (**A**) or methamphetamine (**B**) in saline (SAL; circles) or methamphetamine (METH; squares)-exposed mice. Exposure to methamphetamine significantly increased the distance travelled in mice after both saline (**A**) and methamphetamine challenge (**B**). In response to the METH challenge, METH-exposed TAT+ mice travelled significantly more than METH-exposed TAT− mice (**B**), suggesting enhanced methamphetamine sensitization. Data are expressed as Mean ± SEM (SAL challenge: n=7–9, METH challenge n=11–14). * $p < 0.05$, ** $p < 0.01$, *** $p < 0.001$ between TAT− and TAT+ mice exposed to methamphetamine during the acquisition phase. ### $p < 0.001$ between mice exposed to saline or methamphetamine during the acquisition phase.

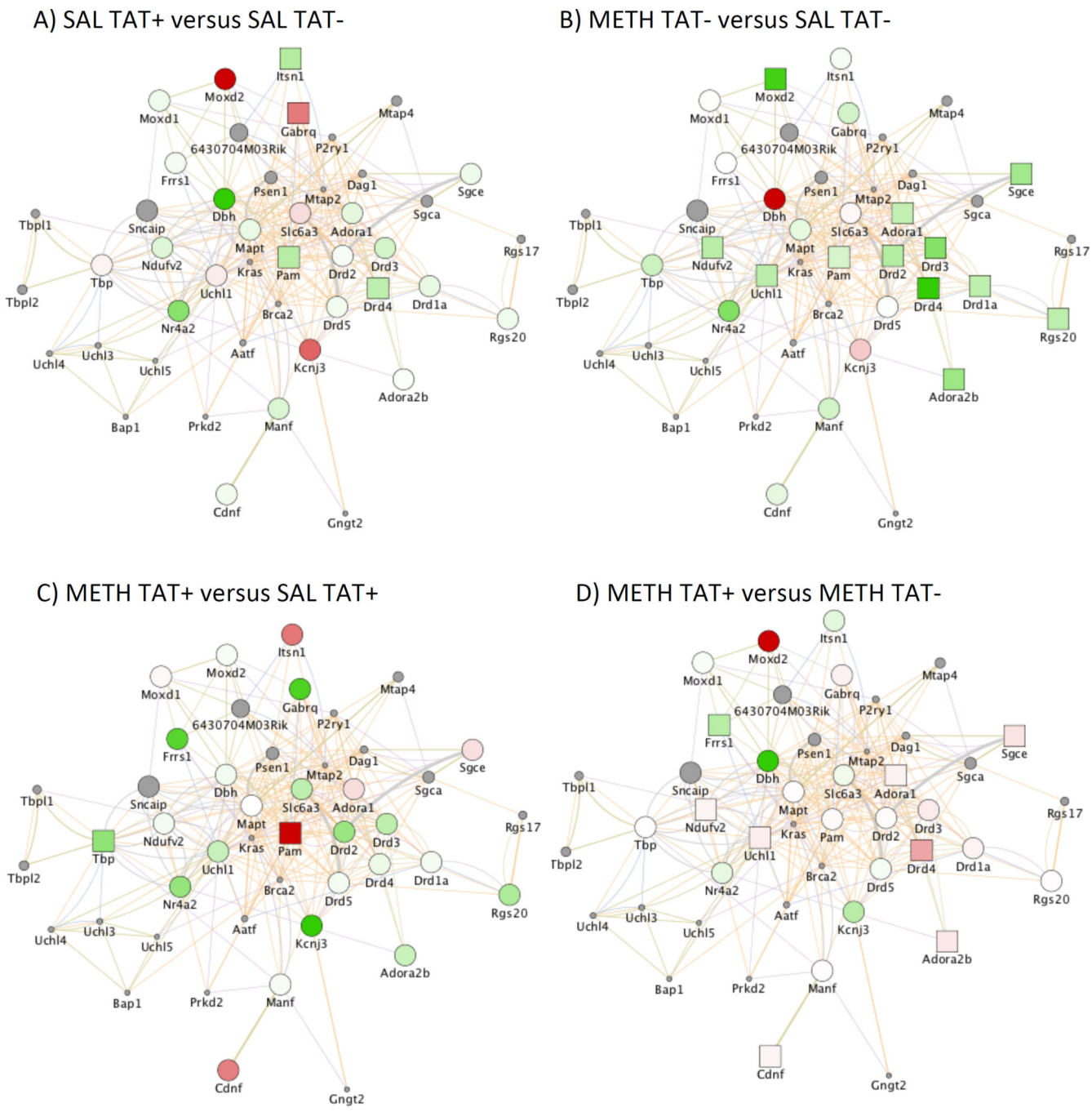

Figure 3. Gene networks associated with the dopaminergic system

Gene changes induced by TAT expression in the brain after exposure to saline (SAL) or methamphetamine (METH) (n=5) in mice challenged with METH. A) Differences between TAT− and TAT+ mice exposed to SAL and challenged with METH. B) Differences between METH and SAL exposure in TAT− mice challenged with METH. C) Differences between METH and SAL exposure in TAT+ mice challenged with METH. D) Differences between TAT− and TAT+ mice exposed to METH and challenged with METH. Orange line connectors represent genes with shared protein domains or pathway interactions, and gray

line connectors represent genes that are co-expressed or co-localized. Green colored shapes represent down regulated genes and Red colored shapes represents upregulated genes. Gray colored circles represent genes in the identified network that were not represented in the Agilent gene array platform. Squares represent $p < 0.05$ between two assigned groups.

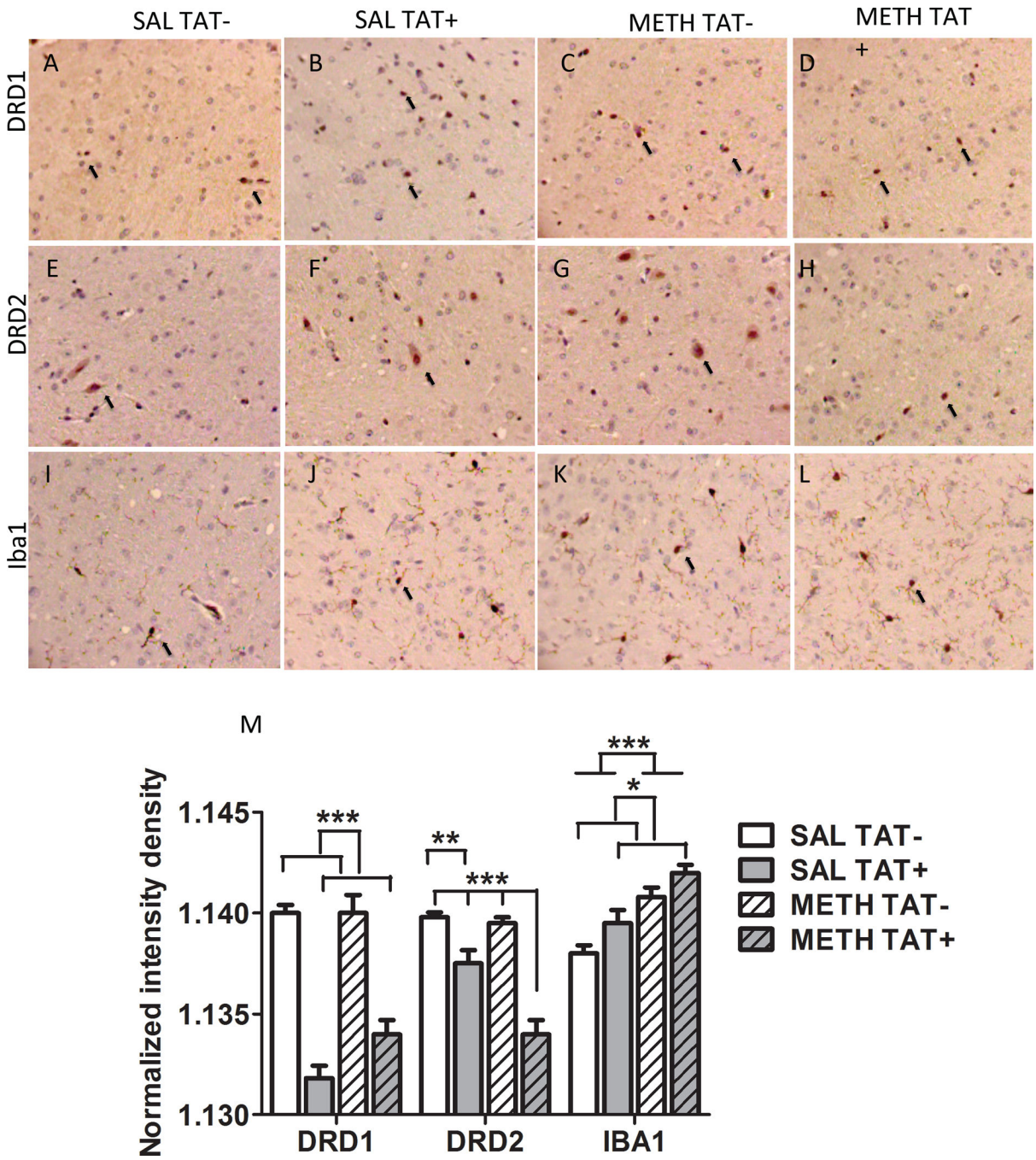

Figure 4. Caudate putamen dopamine receptors expression and IBA-1 expression

Immunohistochemistry on paraffin embedded sections was utilized examine the protein distribution and levels of dopamine receptor D1 (A, B, C, D), dopamine receptor D2 (E, F, G, H), as well as of IBA-1 (I, J, K, L) in SAL TAT− (A, E, I), SAL TAT+ (B, F, J), METH TAT− (C, G, K), and METH TAT+ (D, H, L) mice. Representative positive cells in the 40× magnification images were labeled with a black arrow. (M) Normalized intensity density was calculated in ImageJ. Data are expressed as Mean ± SEM (n=5). * $p < 0.05$, ** $p < 0.01$, *** $p < 0.001$

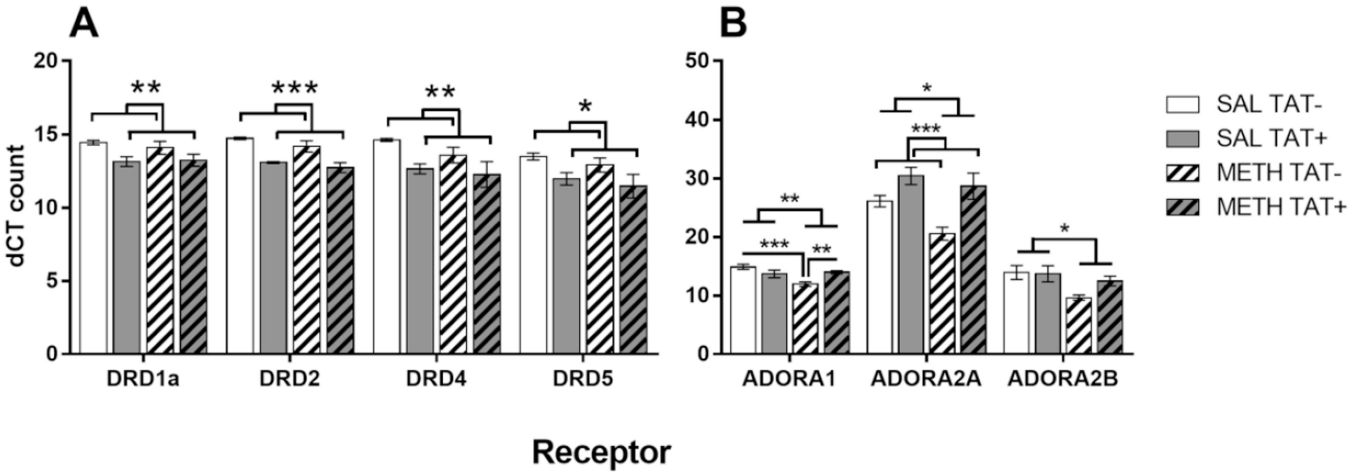

Figure 5. Nucleus accumbens dopamine and adenosine receptor expression

Effects of TAT protein expression on nucleus accumbens dopamine receptor (DRD; **A**) and adenosine receptor (ADORA; **B**) expression in response to methamphetamine challenge after exposure to saline (SAL) or methamphetamine (METH). TAT expression, regardless of methamphetamine exposure decreased the expression of all DRDs (**A**). Methamphetamine exposure, regardless of TAT expression, decreased the expression of the ADORAs (**B**). TAT expression increased levels of ADORA2A and prevented the reduction of ADORA1 by methamphetamine exposure. Data are expressed as Mean ± SEM (n=5). * $p < 0.05$, ** $p < 0.01$, *** $p < 0.001$

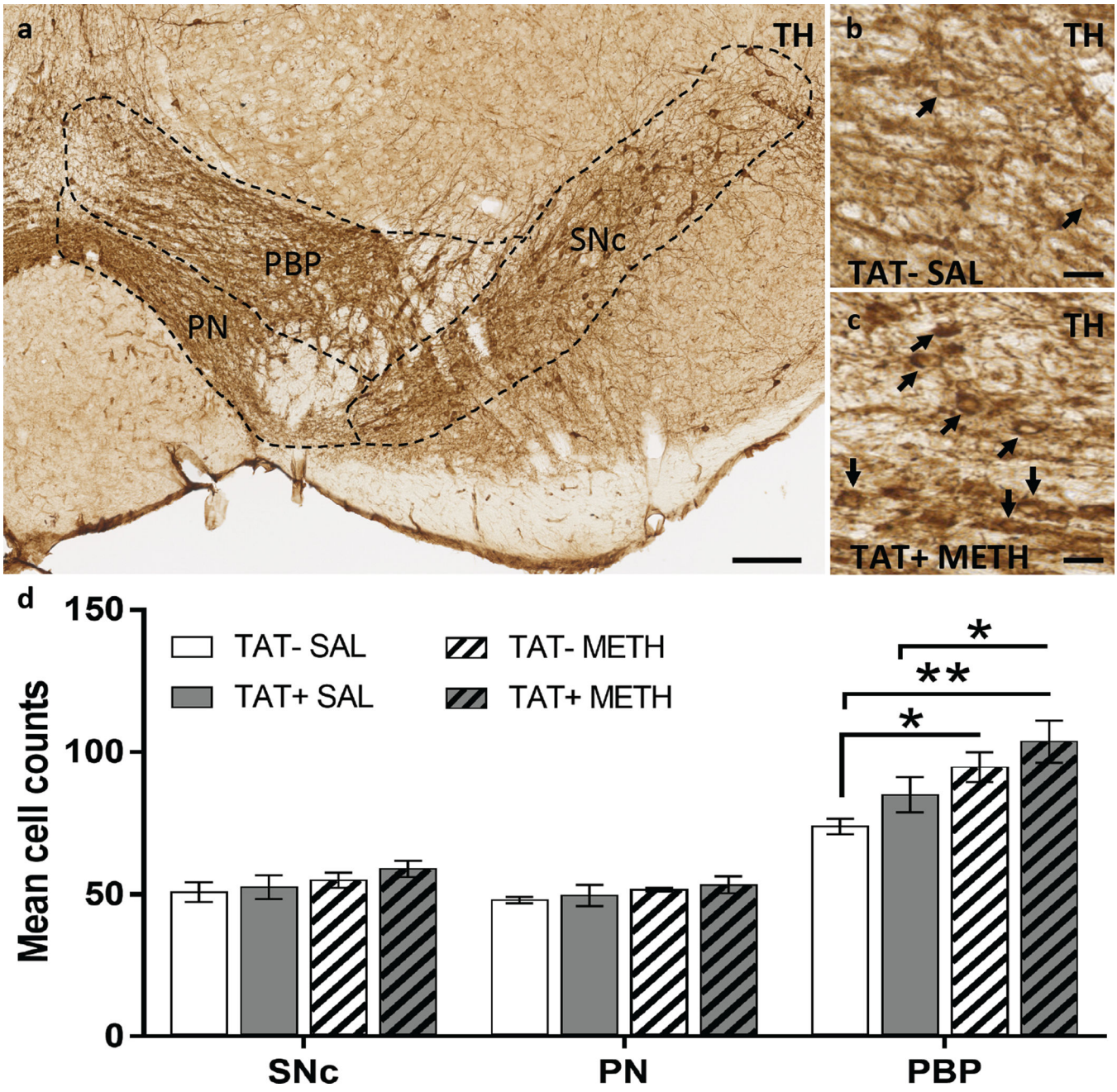

Figure 6. Recruitment of reserve pool neurons to a dopaminergic phenotype

A. Horizontal midbrain section immunostained for tyrosine hydroxylase (TH), showing the substantia nigra pars compacta (SNc) and ventral tegmental subregions (perinigral, PN; parabrachial pigmented, PBP). **B–C.** Representative images of the VTA sectioned through the PBP of a TAT− SAL mouse **(B)** and a TAT+ METH mouse **(C)**; black arrows indicate TH+ neurons. **D.** Graph showing the effects of TAT protein expression (TAT− and TAT+) on (TH)-positive cell number (mean cell count per hemi section) after prior exposure to saline or to methamphetamine. Both TAT expression and prior methamphetamine exposure tended to increase TH-positive cell numbers in the PBP with combined TAT expression and prior

methamphetamine exposure producing the greatest number of TH-positive cells. Data are expressed as Mean ± SEM (n=4). Scale bars: a, 100 μm; b-c, 10 μm). * $p < 0.05$, ** $p < 0.01$.

Table 1

Neurotransmitter levels in the nucleus accumbens after saline challenge.

	TAT−/SAL		TAT+/SAL		TAT−/METH		TAT+/METH	
	Mean	**SEM**	**Mean**	**SEM**	**Mean**	**SEM**	**Mean**	**SEM**
Adrenergic system								
NE	257.60	62.33	199.83	48.32	195.89	25.87	184.50	36.11
Dopamine system								
DA	12428.6	433.0	12850.1	235.3	12519.4	637.5	12925.5	497.6
DOPAC	1153.38	42.17	1131.50	23.86	1206.70	35.34	1173.09	45.79
3-MT	445.79	34.23	397.04	25.70	413.85	26.63	399.51	25.01
HVA	1131.4	47.88	1115.8	63.24	1125.8	50.71	1197.4	43.43
DOPAC/DA	0.0931	0.0032	0.0882	0.0020	0.0977	0.0037	0.0912	0.0032
HVA/DA	0.0910	0.0022	0.0866	0.0035	0.0904	0.0023	0.0932	0.0036
3-MT/DA	0.0358	0.0021	0.0310	0.0022	0.0341	0.0032	0.0312	0.0022
DOPAC/HVA	1.0289	.0505	1.0276	0.0422	1.0794	0.0254	0.9906	0.0579
Serotonin system								
5-HT	744.94	46.22	686.89	45.14	703.56	41.51	708.25	28.16
5-HIAA	431.29	26.36	412.39	31.06	422.94	27.96	435.21	34.57
5-HIAA/5-HT	0.5839	0.0339	0.6081	0.0494	0.6038	0.0256	0.6153	0.0415
Amino acids								
GLU	1563.10	53.26	1598.64	89.98	1621.36	34.81	1619.59	57.45
GABA	284.24	26.78	242.07	21.61	245.71	7.64	242.94	17.72
Glutamine	1286.16	66.95	1394.61	183.40	1283.28	111.88	1310.21	107.90
GLU/GABA	5.74	0.47	6.87	0.65	6.65	0.24	6.92	0.54
Gln/GLU	0.8253	0.0398	0.8724	0.1015	0.7914	0.0654	0.8245	0.0869

SAL, saline exposure; METH, methamphetamine exposure; SEM, standard error of the mean; NE, norepinephrine; DA, dopamine; DOPAC, dihydroxyphenylacetic acid; 3-MT, 3-methoxytyramine; HVA, homovanillic acid; 5-HT, serotonin; 5-HIAA, 5-hydroxy-indoleacetic acid; GLU, glutamate; GABA, γ-aminobutyric acid; Gln, glutamine. (n=7–9).

Table 2

Neurotransmitter levels in the nucleus accumbens after methamphetamine challenge.

	TAT−/SAL		TAT+/SAL		TAT−/METH		TAT+/METH	
	Mean	**SEM**	**Mean**	**SEM**	**Mean**	**SEM**	**Mean**	**SEM**
Adrenergic system								
NE	200.62	25.88	256.00	61.29	293.23	46.19	378.88	106.91
Dopamine system								
DA	11698.0	1058.86	12733.2	909.38	13888.6	744.36	12503.3	846.17
DOPAC	731.56	77.21	784.01	64.40	808.80	41.55	764.25	52.11
3-MT	477.18	31.26	539.01	32.63	534.03	19.69	500.37	36.89
HVA	769.66	43.29	835.12	34.43	888.12	57.26	896.02	45.13
DOPAC/DA	0.0627	0.0026	0.0617	0.0026	0.0585	0.0019	0.0614	0.0024
HVA/DA	0.0682	0.0036	0.0669	0.0027	0.0642	0.0033	0.0727	0.0041
3-MT/DA	0.0422	0.0024	0.0427	0.0014	0.0393	0.0022	0.0401	0.0015
DOPAC/HVA	0.9393	0.0636	0.9352	0.0545	0.9242	0.0393	0.8570	0.0496
Serotonin system								
5-HT	735.50	45.03	738.48	38.02	800.66	36.27	833.68	78.32
5-HIAA	320.03	25.83	331.25	22.42	368.01	29.37	361.21	36.86
5-HIAA/5-HT	0.4336	0.0252	0.4530	0.0315	0.4611	0.0326	0.4456	0.0484
Amino acids								
GLU	1468.38	48.65	1362.54	66.52	1440.24	51.14	1359.81	79.59
GABA	261.89	20.10	284.40	20.39	301.53	21.95	340.87	44.71
Glutamine	1175.48	46.65	1172.80	74.56	1337.87	105.94	1385.66	164.16
GLU/GABA	5.93	0.54	5.07	0.52	4.97	0.35	4.59	0.81
Gln/GLU	0.8117	0.0522	0.8708	0.0601	0.9276	0.0622	1.0332	0.1244

SAL, saline exposure; METH, methamphetamine exposure; SEM, standard error of the mean; NE, norepinephrine; DA, dopamine; DOPAC, dihydroxyphenylacetic acid; 3-MT, 3-methoxytyramine; HVA, homovanillic acid; 5-HT, serotonin; 5-HIAA, 5-hydroxy-indoleacetic acid; GLU, glutamate; GABA, γ-aminobutyric acid; Gln, glutamine. (n=7–10).